Proceedings of the Canadian Society for Mechanical Engineering International Congress
32nd Annual Conference of the Computational Fluid Dynamics Society of Canada
Canadian Society of Rheology Symposium
CSME-CFDSC-CSR 2025
May 25–28, 2025, Montréal, Québec, Canada

Energy, Exergy, and Exergoeconomic Analyses of Solar-Powered Cooling Systems for Data Centers in Montreal: A Comparative Study of Three Phase Change Materials

Daryoush Dadpour[a,c,*], Mahdi Deymi-Dashtebayaz[b], Sébastien Poncet[c], Martin Agelin-Chaab[a], Horia Hangan[a], Hassan Peerhossaini[a,d]

[a] Clean Energy Research Laboratory (CERL), FEAS, Ontario Tech University, Oshawa, Ontario, Canada
[b] Center of Computational Energy, Department of Mechanical Engineering, Hakim Sabzevari University, Sabzevar, Iran
[c] Department of Mechanical Engineering, Université de Sherbrooke, Sherbrooke, Canada
[d] Matière et Systèmes Complexes Lab., Université de Paris, Paris, France
also Department of Civile & Environmental Engineering, Western University, London, Canada

*Daryoush.Dadpour@ontariotechu.net

Abstract— This research explores the creation of a sophisticated solar-powered cooling system designed specifically for data centers, tackling the issue of fluctuating solar energy availability. The system features thermal energy storage (TES) enhanced with phase change materials (PCMs) to maintain a stable thermal output when solar power is not available. The study assesses three PCMs—Adipic acid, Dimethyl terephthalate, and Suberic acid—considering factors like density, latent heat of fusion, melting point, and specific heat capacity. Dimethyl terephthalate emerged as the top performer in terms of exergy efficiency, achieving as high as 80% during the PCM charging phase, which underscores its effectiveness for the intended application.

Keywords: Data center, Thermal energy storage, Phase change material, Solar energy, Absorption chiller.

I. INTRODUCTION

Solar energy, being dependent on weather conditions and characterized by its intermittent nature, lacks the reliability required for continuous operation throughout the day [1]. This limitation presents significant challenges, particularly for applications that demand a steady supply of thermal energy within specific temperature ranges. For instance, in refrigeration systems such as absorption chillers, which operate within a temperature range of 100 to 130°C, maintaining a stable thermal energy supply is essential. To overcome this challenge, the integration of thermal energy storage (TES) systems has become a key strategy for enhancing operational stability and maximizing energy efficiency [2]. Therefore, utilizing TES can be an effective solution for the sustainable utilization of solar energy. Researchers have examined TES from various perspectives. Belmonte et al. [3] explored the use of phase-change materials (PCMs) in the heat rejection loops of residential solar absorption cooling systems in Spain. They analyzed the replacement of conventional wet cooling towers with dry coolers and PCM-based thermal energy storage (TES) systems using TRNSYS simulations. Two configurations were evaluated for summer performance. Their findings revealed a performance boost of one unit with a 1 m³ PCM-based TES in mild, humid climates but noted trade-offs such as a 7-13% drop in chiller efficiency and a 21-38% decrease in cooling energy output. The study highlighted the dual benefits and drawbacks of PCM-TES integration. Abbasi et al. [4] optimized a solar absorption chiller in Tehran's Mehrabad region using exergoeconomic principles and a genetic algorithm (GA). They incorporated a PCM-based TES system to improve chiller operation during low solar radiation periods, especially at night. Optimization led to a 2.06% increase in investment costs for the main system, and the TES system extended the payback period from 0.61 to 1.13 years. This research emphasized the role of PCM-based TES in improving solar chiller performance, albeit with higher costs and longer payback durations. Mashhour et al. [5]and Alazwari et al. investigated cooling systems in Saudi Arabia, where cooling constitutes 66% of building energy use. They developed a transient thermal model using the enthalpy-porosity technique to assess PCM-integrated walls and ceilings under high solar irradiance. Their system, combining an air-handling unit (AHU) and an absorption chiller, demonstrated a 7.13% reduction in heat gain and 47.3 kWh/m².year energy savings with PCMs. Adding a recovery unit (RU) cut energy demand by 8.38%, totaling a 14.6% reduction in AHU energy

use (111.1 kWh/m².year saved). This study showcased the potential of combining PCMs and RUs for energy efficiency in buildings. Huang et al. [6] upgraded a 1000-liter solar cooling and heating plant to address issues with chiller cycling and high electricity consumption. The retrofit added a shell-and-tube heat exchanger with a 64°C melting-point PCM and optimized control. Post-upgrade, chiller on-times decreased by 33.5%, uptime rose by 65%, and the solar fraction (SF) during cooling improved from 50.9% to 75.6%. These changes reduced electricity use by 24.4%, demonstrating the effectiveness of PCM-enhanced systems in stabilizing solar thermal applications. Wei et al. [7] introduced a 24-hour energy harvesting system combining photovoltaic (PV) cells, thermoelectric generators (TEG), and PCMs, known as the PV-TEG-PCM system. This setup used PV cells for solar electricity, TEG for heat-to-power conversion, and PCMs for thermal regulation and nighttime cooling. Optimized for a 38°C PCM phase change temperature and 30 mm thickness, the system achieved a PV efficiency of 19.6%, TEG efficiency of 1.2%, and overall efficiency of 20.8%. Field tests demonstrated energy generation both day and night, highlighting its promise for urban applications like solar-powered streetlights.

In previous studies, thermal energy storage (TES) has been investigated from various perspectives. This research aims to analyze and compare three different materials for their suitability in thermal energy storage. The system is designed to provide cooling for a data center. To model the system, energy, exergy, and exergoeconomic analyses have been employed.

II. SYSTEM DESCRIPTION

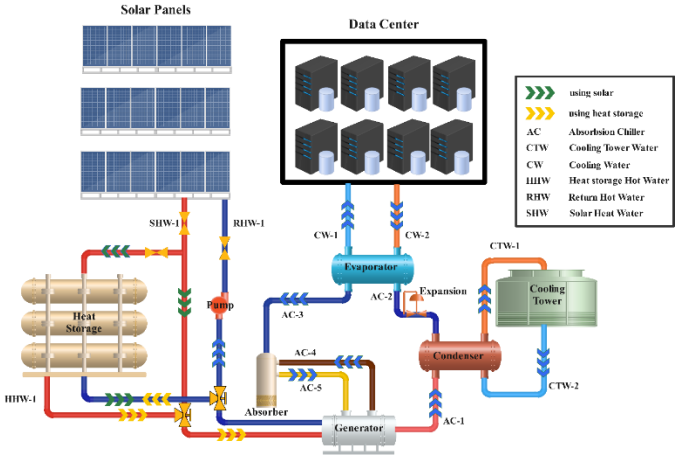

Fig. 1. Schematic diagram of the proposed cycle

The cycle described in this study is designed to meet the cooling requirements of a data center using a direct-fired absorption chiller with lithium bromide-water as the working fluid. Solar energy powers the chiller during the day, while phase-change materials (PCMs) provide stored heat at night. Three types of PCMs with distinct thermodynamic properties are used, as detailed in Table 1. Solar energy is transferred to water via CPVT plates, heating it to approximately 170°C at SHW-1. The fluid is divided, with one portion heating the PCM and the other supplying the chiller, before returning to the panels via RHW-1 after heat exchange. PCM charging occurs during the day, and discharging happens at night, represented by green and yellow arrows, respectively. In the generator, diluted lithium bromide absorbs heat, evaporating water at around 70°C (AC-1), which then condenses into liquid (AC-2) and cools to 4°C in the evaporator. The evaporated water is reabsorbed by lithium bromide, completing the cycle. The cycle used in this paper is illustrated in Fig. 1.

Table. 1. Input parameters for the proposed system.

PCM solid density (kg/m^3)	Adipic acid	1360
	Dimethyl terephthalate	1290
	Suberic acid	1020
PCM phase change enthalpy (kJ/kg)	Adipic acid	260
	Dimethyl terephthalate	170
	Suberic acid	245
PCM melting temperature (℃)	Adipic acid	151
	Dimethyl terephthalate	142
	Suberic acid	141
Specific heat (J/kg.K)	Adipic acid	1550
	Dimethyl terephthalate	1670
	Suberic acid	1579

III. GOVERNING EQUATIONS

For the energy, exergy, and exergoeconomic evaluation of the suggested cogeneration system, the following assumptions were considered:

- The components of the system are considered to be adiabatic.
- Changes in kinetic and potential energies are disregarded.
- Pressure losses in the heat exchangers are deemed insignificant.
- Chemical reactions are excluded from consideration.

Based on the above assumptions, the mass and energy balance equations for the components of the system are formulated as follows [8]:

$$(\sum_{out} \dot{m} \cdot h) - (\sum_{in} \dot{m} \cdot h) = \dot{Q}_{C.V.} - \dot{W}_{C.V.} \quad (1)$$

$$(\sum_{out} \dot{m}) - (\sum_{in} \dot{m}) = 0 \quad (2)$$

$$(\sum_{\text{out}} \dot{\text{m}} \cdot \text{ex}) - (\sum_{\text{in}} \dot{\text{m}} \cdot \text{ex}) + \dot{EX}_{des,C.V.} = \dot{EX}_{Q,C.V.} - \dot{EX}_{W,C.V.} \quad (3)$$

The equations below were employed to model the solar collector [9].

$$\eta_{\mathrm{PTC}} = 0.75 - [0.000045 \cdot (T_{RHW-1} - T_{\mathrm{amb}})] - \left[0.039 \cdot \left(\frac{T_{RHW-1} - T_{\mathrm{amb}}}{G_B}\right)\right] - \left[0.001672 \cdot G_b \cdot \left(\frac{T_{RHW-1} - T_{\mathrm{amb}}}{G_B}\right)^2\right] \quad (4)$$

In Equation (4), T_{RHW-1} (°C) represents the inlet temperature of the collector, T_{amb} denotes the ambient temperature, and G_B (W/m²) refers to the beam solar radiation, which changes on an hourly basis.

Additionally, the heat generation by PTC collectors is determined using Equation (5) [9].

$$\dot{Q}_{use} = A_{PTC} . \eta_{PTC} . G_B \quad (5)$$

In this context, $\dot{Q}_{use}$ represents the thermal energy in kilowatts (kW), η_{PTC} denotes the thermal efficiency, and A_{PTC} is the area of the PTC collectors measured in square meters (m²).

The exergy rate of the solar energy for the PTC, denoted as $\dot{EX}_{PTC}$, is computed using Equation 6 [10]:

$$\dot{EX}_{PTC} = A_{PTC} . G_B \left(1 - \frac{4}{3}\frac{T_{amb}}{T_{Sun}} + \frac{1}{3}\left(\frac{T_{amb}}{T_{Sun}}\right)^4\right) \quad (6)$$

TES and PCM:

This section also provides a detailed analysis of thermal calculations related to the Thermal Energy Storage (TES) and Phase Change Materials (PCM). The capacity of TES is determined using Equation 7 [41,42], which directly links the heat gained by TES to the solar energy absorbed by the PCM. The specifics of the equations for PCM are outlined in Equations 8 through 10.

$$\rho V_{TES} C_p \frac{dT_{TES}}{dt} = \dot{m}_{SHW-1}(T_{SHW-1} - T_{TES}) + \dot{m}_{RHW-1}(T_{RHW-1} - T_{TES}) - \overbrace{UA_{TES}(T_{TES} - T_{amb})}^{\dot{Q}_{lose}} \quad (7)$$

In this context, ρ indicates the density of the PCM (kg/m³), V is the volume of the TES (m³), Cp represents the specific heat capacity of the PCM (kJ/kg.K), U denotes the heat transfer coefficient of the TES walls (kJ/m².K), and A is the outer surface area of the TES (m²). For the purposes of this study, the heat loss $\dot{Q}_{lose}$ is considered to be zero.

Equations (8) and (9) are used to calculate the minimum and maximum energy values for the PCM, denoted as $E_{pcm_{min}}$, and $E_{pcm_{max}}$ respectively.

$$E_{pcm_{min}} = [(1 - \varphi) . V . \rho_w . c_w . T_m] + [\varphi . V . \rho_{pcm} . c_{pcm} . T_m] \quad (8)$$

$$E_{pcm_{max}} = E_{pcm_{min}} + [\varphi . V . \rho_{pcm} . h_{pcm}] \quad (9)$$

In this analysis, φ signifies the volume fraction of the PCM within the TES system, V represents the volume of the tank, ρ_w is the density of water, c_w refers to the specific heat capacity of water, T_m denotes the melting temperature of the PCM, and h_{pcm} is the enthalpy of the PCM.

Additionally, a critical aspect studied in relation to PCMs is the liquid fraction, which is defined as follows:

$$f = \begin{cases} 0 & if \;\; E(t) < E_{pcm_{min}} \\ \dfrac{E(t) - E_{pcm_{min}}}{E_{pcm_{max}} - E_{pcm_{min}}} & if \;\; E_{pcm_{min}} \le E(t) \le E_{pcm_{max}} \\ 1 & if \; E(t) \ge E_{pcm_{max}} \end{cases} \quad (10)$$

When $0 < f < 1$, it indicates that the PCM is in a transitional phase, either melting or freezing, and the temperature within the tank remains constant at the melting temperature of the PCM.

Eco-exergy:

Eco-exergy analysis combines exergy and economic assessments to evaluate the performance of energy systems. It utilizes thermodynamic efficiencies, economic principles, and impact factors to provide a comprehensive view of the system's performance. This approach offers crucial insights into the costs associated with component usage, exergy destruction, and thermodynamic inefficiencies. Equations (13-16) elaborate on the specific relationships used in this eco-exergy analysis [8].

$$\sum \dot{C}_{in,i} + \dot{C}_{Q,i} + \dot{Z}_i = \sum \dot{C}_{out,i} + \dot{C}_{W,i} \quad (13)$$

$$\dot{C}_{in} = c_{in} \times \dot{Ex}_{in} \quad (14)$$

$$\dot{C}_{out} = c_{out} \times \dot{Ex}_{out} \quad (15)$$

$$\dot{C}_Q = c_Q \times \dot{Ex}_Q \quad (16)$$

Equation 13 calculates the exergetic cost rate of the system, where $\dot{C}_{in}$ and $\dot{C}_{out}$ denote the exergetic cost rates at the inlet and outlet, respectively. These rates are calculated using Equations (14) and (15), which consider the inlet and outlet exergy rates along with their respective costs per unit of exergy. Equation 16 is then used to determine the exergetic cost rates associated with the heat transfer, represented as $\dot{C}_Q$. Subsequently, Equations (17-20) aggregate the total cost rate $\dot{Z}_i$ by adding the capital investment cost rate $\dot{Z}^{CI}$ and the operational and maintenance cost rate $\dot{Z}^{OM}$ [8].

$$\dot{Z}_{tot,i} = \dot{Z}_i^{CI} + \dot{Z}_i^{O\&M} \quad (17)$$

$$\dot{Z}_i^{CI} = (\frac{CRF}{\tau}) Z_i \quad (18)$$

$$CRF = \frac{i(1+i)^n}{(1+i)^n - 1} \quad (19)$$

$$\dot{Z}_i^{OM} = \gamma_i Z_i \quad (20)$$

IV. VALIDATION

The findings presented in this article are compared with experimental data [11] in Figure 2, which illustrates the temperature variations of the PCM over time. As demonstrated, the final temperature closely matches the experimental results.

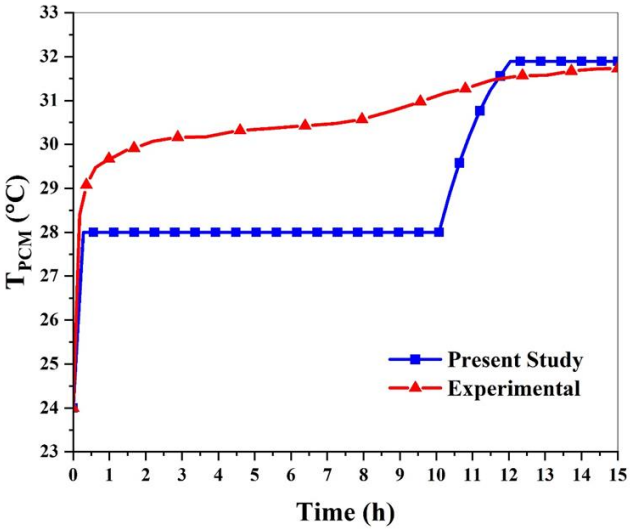

Fig. 2. Validation of the PCM for the present model

V. RESULTS

This study focuses on fulfilling the cooling demands of a data center using solar power. Energy stored in the Phase Change Material (PCM) is utilized during nighttime when solar energy is not available. For a comprehensive analysis, data from a representative day in each season is examined, and the outcomes are discussed accordingly. The study also evaluates three different types of PCMs to determine the most effective option by comparing their performances.

Figure 3 displays the fluctuations in radiation and temperature over a single day for each season. The peak solar radiation is recorded in summer (August), while the lowest occurs in autumn (November). Winter (February) experiences the shortest period of solar radiation, with sunrise around 8 a.m. and sunset near 6 p.m. Consistent with expectations, the highest ambient temperatures are recorded in the sequence of summer (August), followed by spring (May), autumn (November), and winter (February).

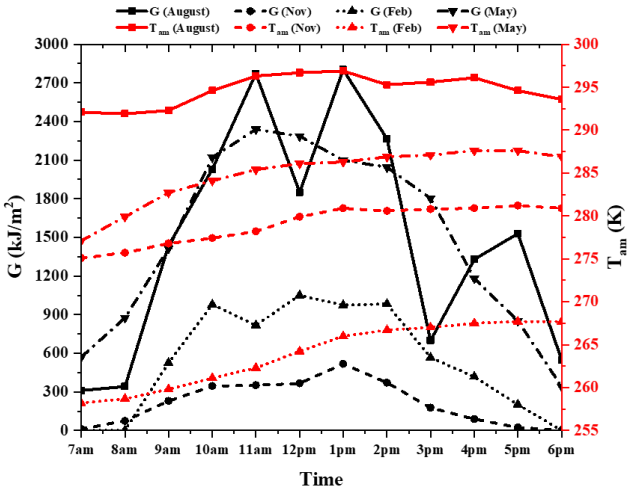

Fig. 3. Variations in solar radiation and ambient temperature throughout a day in four different months in Mirabel station.

Figure 4 illustrates the impact of variations in T_{AC-1} on the Coefficient of Performance (COP). Given that the chiller model is designed to assume a constant heat supply regardless of the PCM type or season, the COP value remains unchanged across different seasons and PCM types. Consequently, Fig. 4 displays only a single line representing the COP.

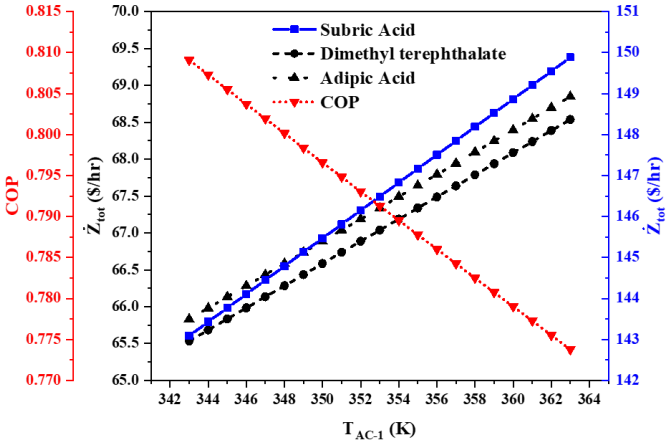

Fig. 4. Variation of the total system cost and COP with the outlet steam temperature of the generator.

Figure 5 illustrates T_{SHW-1} alongside exergy efficiency. The results indicate that exergy efficiency increases with the rise in T_{SHW-1}. Furthermore, among the analyzed PCMs, Dimethyl exhibits the highest exergy efficiency.

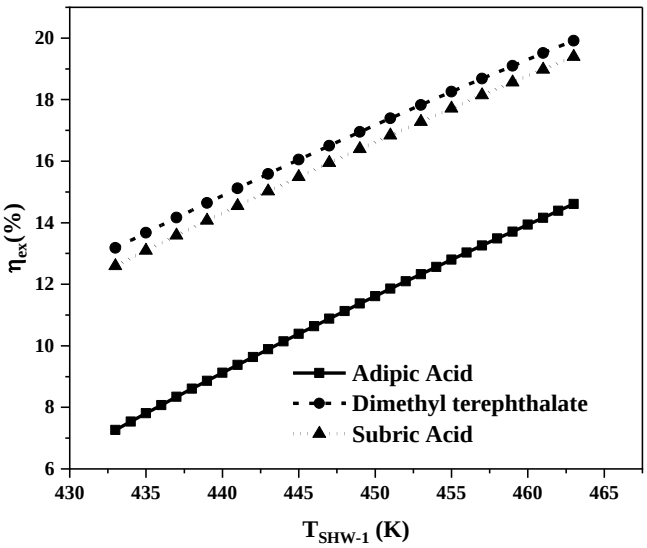

Fig. 5. Variation of the system exergy efficiency with the outlet temperature of the solar panel

As mentioned earlier, the PCM provides the necessary heat to the chiller during periods without sunlight. To fulfill this role, the mass of the PCM must be adequate to meet the thermal demands. Consequently, the required mass varies depending on the heat capacity of each specific PCM. During daylight, the PCM absorbs heat and melts completely; then, at night, this stored heat is utilized, leading to the re-solidification of the PCM. This process is accompanied by consistent temperature patterns: as the PCM absorbs heat, its temperature increases to the melting point and remains steady. While releasing heat at night, the PCM's temperature stays constant until it fully solidifies, after which it begins to drop. Figure 6 displays the variations in temperature and melted mass throughout the day for three different PCM types.

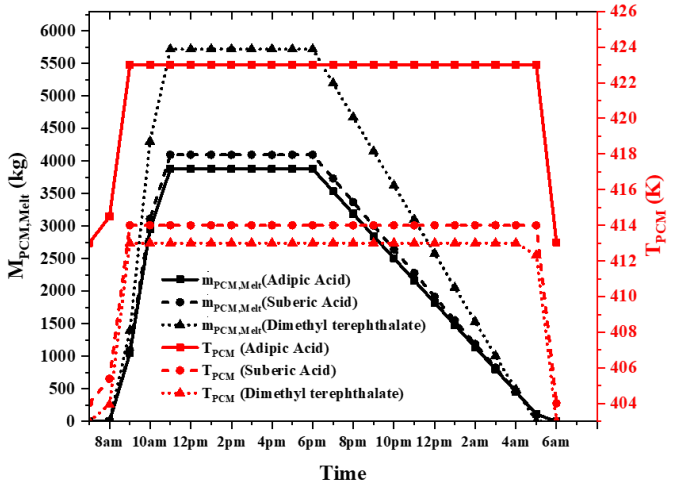

Fig. 1 Variations in the mass and temperature of the PCM over the day and night cycle.

During the day, the solar heat absorbed is divided between two main components of the cycle: charging the PCM in one part while supporting the chiller in the other. Figure 7 illustrates the mass flow rate generated from the solar panel, as well as the portion of the flow directed towards the PCM over the course of a day. The discharge from the solar panel reaches its peak in August, corresponding to the highest solar radiation levels, and hits its lowest point in November, when solar radiation is minimal. The solar energy allocated for charging the PCM continues until it is fully charged; after this point, the flow directed to the PCM drops to zero, as depicted in Figure 7.

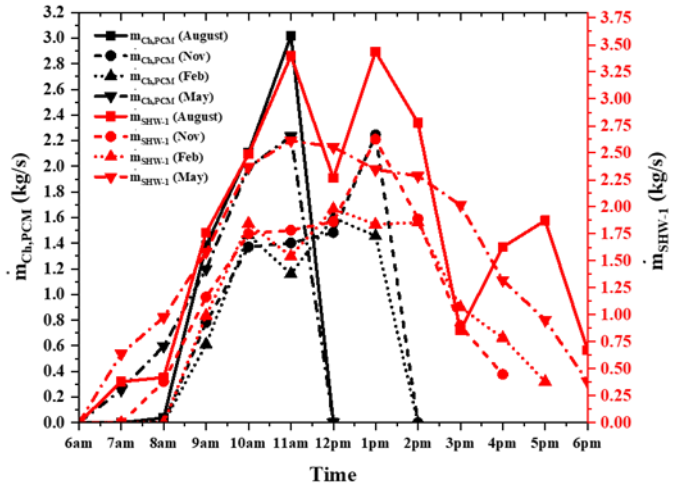

Fig. 2 Changes in the PCM mass flow rate and solar panel output over the course of a day.

VI. Conclusion

This research successfully addresses the challenges of designing an efficient and sustainable cooling system for data centers powered by solar energy, integrating advanced thermal energy storage (TES) systems with phase change materials (PCMs). In this study, the system was analyzed using energy, exergy, and exergoeconomic analyses, leading to the following key findings and insights:

- The integration of TES with PCMs has significantly enhanced system resilience by ensuring a continuous and stable supply of thermal energy during periods without solar exposure. This reliability is crucial for data center operations, which have dynamic cooling needs and are highly sensitive to any disruptions. The system's ability to adapt to fluctuating solar radiation levels throughout the year was evident, with the most efficient solar energy utilization occurring during the summer months. Additionally, the application of transient simulations that incorporate high-resolution meteorological data provided further validation of the system's effectiveness under real-world conditions.
- The highest system cost arises from the expensive PCM, specifically suberic acid, while the costs for the other two PCMs are approximately similar.
- Due to the lower phase change enthalpy of Dimethyl compared to the other two PCMs, it necessitates a greater

mass to supply the required heat for the chiller during the night.

VII. References

[1] Q. Xuan *et al.*, "Combined daytime radiative cooling and solar photovoltaic/thermal hybrid system for year-round energy saving in buildings," *Energy*, vol. 304, 132178, 2024.

[2] M. Kheir Abadi, V. Davoodi, M. Deymi-Dashtebayaz, and A. Ebrahimi-Moghadam, "Determining the best scenario for providing electrical, cooling, and hot water consuming of a building with utilizing a novel wind/solar-based hybrid system," *Energy*, vol. 273, 127239, 2023.

[3] J. F. Belmonte, M. A. Izquierdo-Barrientos, P. Eguía, A. E. Molina, and J. A. Almendros-Ibáñez, "PCM in the heat rejection loops of absorption chillers. A feasibility study for the residential sector in Spain," *Energy Build*, vol. 80, pp. 331–351, 2014.

[4] A. A. Godarzi, M. Jalilian, J. Samimi, A. Jokar, and M. A. Vesaghi, "Design of a PCM storage system for a solar absorption chiller based on exergoeconomic analysis and genetic algorithm," *International Journal of Refrigeration*, vol. 36, no. 1, pp. 88–101, 2013.

[5] M. A. Alazwari, N. H. Abu-Hamdeh, A. Khoshaim, K. H. Almitani, and A. Karimipour, "Using phase change material as an energy-efficient technique to reduce energy demand in air handling unit integrated with absorption chiller and recovery unit–Applicable for high solar-irradiance regions," *Journal of Energy Storage*, vol. 42, 103080, 2021.

[6] L. Huang, U. Piontek, L. Zhuang, R. Zheng, and D. Zou, "Retrofitting of a solar cooling and heating plant by employing PCM storage and adjusting control strategy," *Applied Energy*, vol. 368, 123462, 2024.

[7] W. Wei *et al.*, "A continuous 24-hour power generated PV-TEG-PCM hybrid system enabled by solar diurnal photovoltaic/thermal conversion and nocturnal sky radiative cooling," *Energy Conversion & Management*, vol. 321, 119086, 2024.

[8] M. Tavana, M. Deymi-Dashtebayaz, D. Dadpour, and B. Mohseni-Gharyehsafa, "Realistic Energy, Exergy, and Exergoeconomic (3E) Characterization of a Steam Power Plant: Multi-Criteria Optimization Case Study of Mashhad Tous Power Plant," *Water*, vol. 15, no. 17, 2023.

[9] M. Yazdani, M. Deymi-Dashtebayaz, and S. Ghorbani, "Multi-objective optimization and 3E analysis for solar-driven dual ejector refrigeration and phase change material as thermal energy storage," *Applied Thermal Engineering*, vol. 249, 123431, 2024.

[10] V. Davoodi, E. Amiri Rad, M. Akhoundi, and U. Eicker, "Design, optimization, and performance analysis of a solar-wind powered compression chiller with built-in energy storage system for sustainable cooling in remote areas," *Energy*, vol. 312, 133664, 2024.

[11] J. F. Belmonte, P. Eguía, A. E. Molina, J. A. Almendros-Ibáñez, and R. Salgado, "A simplified method for modeling the thermal performance of storage tanks containing PCMs," *Applied Thermal Engineering*, vol. 95, pp. 394–410, 2016.